Article:
M. E. Dokla, E, Kamal Abdel-Aziz, A, Milik, SN et al. (2022) Discovery of a Benzimidazole-based Dual FLT3/TrKA Inhibitor Targeting Acute Myeloid Leukemia. Bioorganic and Medicinal Chemistry, 56. 116596. p. 116596. ISSN: 0968-0896

https://doi.org/10.1016/j.bmc.2021.116596

Discovery of a Benzimidazole-based Dual FLT3/TrKA Inhibitor Targeting Acute Myeloid Leukemia

Eman M. E. Dokla[a,*,†],Amal Kamal Abdel-Aziz[b,c†], Sandra N. Milik[a,d,†], Martin J. McPhillie[d], Saverio Minucci[c,e,¥,*], Khaled A. M. Abouzid[a,f,¥]

[a]*Pharmaceutical Chemistry Department, Faculty of Pharmacy, Ain Shams University, Abbassia, Cairo 11566, Egypt*

[b]*Department of Pharmacology and Toxicology, Faculty of Pharmacy, Ain Shams University, Abbassia, Cairo, 11566, Egypt*

[c]*Department of Experimental Oncology, IEO, European Institute of Oncology IRCCS, Via Adamello 16, 20139, Milan, Italy*

[d]*School of Chemistry, University of Leeds, Leeds LS2 9JT, United Kingdom*

[e]*Department of Biosciences, University of Milan, Milan, 20100, Italy*

[f]*Department of Organic and Medicinal Chemistry, Faculty of Pharmacy, University of Sadat City, Sadat City, 32897, Egypt*

[*]Corresponding author.

E-mail address: emanelawady@pharma.asu.edu.eg (E.M.E. Dokla); Saverio.Minucci@ieo.it (S. Minucci)

[†]These authors have equal contributions.

[¥] These authors are co-senior authors

Abstract

FMS-like tyrosine kinase 3 (FLT3) enzyme overexpression and mutations are the most common molecular abnormalities associated with acute myeloid leukemia (AML). In addition, recent studies investigated the role of tropomyosin receptor kinase A (TrKA) enzyme fusions in promoting AML growth and survival. Based on these premises, targeting both kinases using dual inhibitors would constitute a promising therapeutic approach to target resistant AML. Guided by ligand-based design and structure simplification of the FLT3 inhibitor, quizartinib, we developed a benzimidazole-based small molecule, **4ACP**, that exhibited nanomolar activity against wild-type FLT3, FLT3-Internal tandem duplications (FLT3-ITD), and FLT3-D835Y (FLT3-TKD) mutation (IC_{50} = 43.8, 97.2, and 92.5 nM respectively). Additionally, **4ACP** demonstrated potent activity against colon cancer KM12 cell line (IC_{50} = 358 nM) and subsequent mechanistic deconvolution identified TrKA enzyme as a second plausible target (IC_{50} = 23.6 nM) for our compound. **4ACP** manifested preferential antiproliferative activity against FLT3-ITD positive AML cell lines (MV4-11 IC_{50} = 38.8±10.7 nM and MOLM-13 IC_{50} = 54.9±4.1 nM), while lacking activity against FLT3-ITD negative AML cell lines. Western blot analysis confirmed **4ACP** ability to downregulate ERK1/2 and mTOR signaling downstream of FLT3-ITD in AML cells. Furthermore, **4ACP** prompted apoptotic and necrotic cell death and G0/G1 cell cycle arrest as indicated by cell cycle analysis.

4ACP did not show cytotoxic effects on normal BNL and H9c2 cells and demonstrated decreased activity against c-Kit enzyme, hence, indicating lower probability of synthetic lethal toxicity and a relatively safer profile. In light of these data, **4ACP** represents a novel FLT3/TrKA dual kinase inhibitor for targeted therapy of AML.

Keywords

FLT3; TrKA; dual kinase inhibitor; acute myeloid leukemia; benzimidazole; scaffold hopping

1. Introduction

Acute myeloid leukemia (AML) is a common form of blood cancer resulting from improper differentiation and proliferation of hematopoietic stem cells leading to anemia, infections, and bleeding [1]. Despite the recent progress in understanding the disease and the various treatment methods introduced, bad prognosis persists particularly in adult patients [2]. According to the American Cancer Society report in 2020, 19,940 new cases of AML were diagnosed (32.9% of total leukemia cases) and 11,180 deaths were reported (48.4% of leukemia-related deaths) [3]. AML is a heterogenous disease with diverse underlying molecular abnormalities rather than a single cause [4,5]. Therefore, current research efforts are directed to address AML targetable abnormalities and identify new ones to benefit from AML-tailored anticancer therapy [6,7].

FMS-like tyrosine kinase 3 (FLT3) protein is expressed ordinarily in hematopoietic cells and its activation by FLT3 ligand and subsequent downstream cellular signaling cascade culminates in controlled proliferation, survival, and inhibition of hematopoietic cells differentiation [8]. FLT3-WT is overexpressed in AML [9] and FLT3 gene mutations are the most common genetic variations associated with AML manifesting in one-third of diagnosed patients. Two major FLT3 mutations were identified in AML, FLT3-internal tandem duplications (FLT3-ITD) and FLT3-tyrosine kinase domain point mutations (FLT3-TKD), most commonly D835Y mutation in the activation loop [10–12]. Both mutations cause dimerization and constitutive activation of FLT3 receptor independent of FLT3 ligand binding which lead to uncontrolled proliferation, survival and anti-apoptotic effects of AML cells [4,9,13]. In light of FLT3 involvement and implications in AML, targeting both FLT3-WT and mutated FLT3 represents a promising therapeutic approach for AML-directed therapy [7,9,14].

Numerous small molecule FLT3 tyrosine kinase inhibitors were reported during the last two decades and few of these are currently undergoing clinical trials or were recently approved by FDA for AML [15–17]. These comprise the first-generation inhibitors, sunitinib [18], midostaurin [19], lestaurtinib [20], tandutinib [21], and sorafenib [22] and the second-generation inhibitors, quizartinib [23], gilteritinib [24], and crenolanib [25] (**Figure 1**). FLT3 inhibitors are also classified according to their binding mode to the ATP binding site into, type I inhibitors including sunitinib, midostaurin,

lestaurtinib, gilteritinib, and crenolanib that bind to the active conformation (DFG-in) and type II inhibitors comprising sorafenib, quizartinib, and tandutinib that bind to the inactive conformation (DFG-out) [26–29]. These small molecule TKIs vary greatly in their kinome selectivity, potency, activity on FLT3-mutant forms, and resistance profiles [7,14].

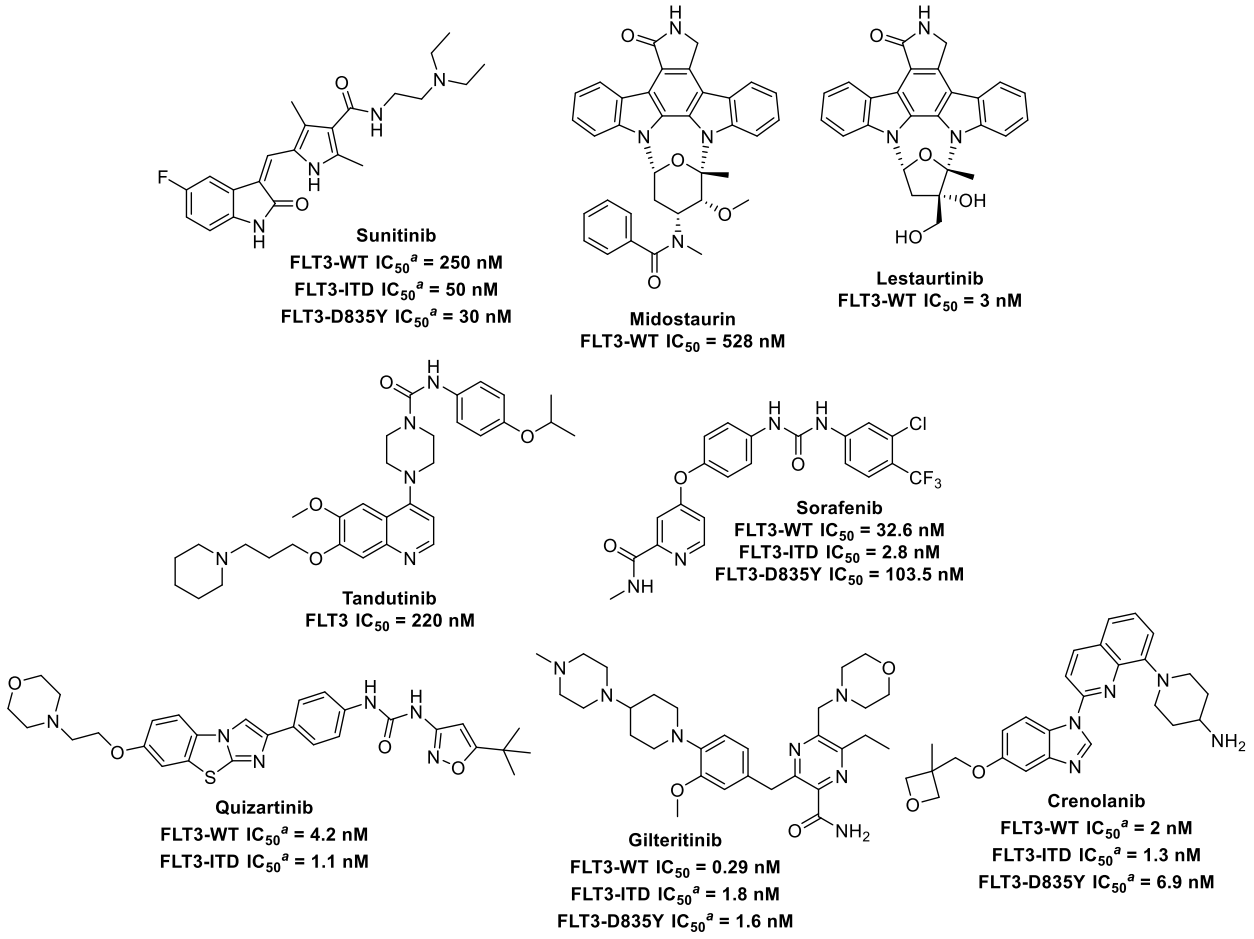

Figure 1. Chemical structures of reported FLT3 kinase inhibitors.
[a]Cell-based assay.

Emergence of resistance to clinically used FLT3 tyrosine kinase inhibitors in AML is a common phenomenon that results in limited response and relapse [7,26,30]. A major cause of this resistance is the acquired point mutations of the FLT3-TKD which affect the binding affinity of selective FLT3 inhibitors particularly type II [31,32]. Accordingly, several approaches were investigated to address these resistance mechanisms which comprise, employing combination therapies [33,34], developing novel FLT3 Inhibitors effective against FLT3-ITD-TKD mutations [35,36], or use of irreversible inhibitors [37].

One approach to target AML heterogeneity and acquired resistance is the development of dual kinase inhibitors which might affect different oncogenic pathways related to AML or inhibit alternate signaling pathways that mediate resistance [38,39]. Of these, the previously mentioned midostaurin is a dual FLT3/SYK inhibitor, lestaurtinib is a dual FLT3/TrKA inhibitor, tandutinib and crenolanib are dual FLT3/PDGFR inhibitors, and gilteritinib is a dual FLT3/AXL inhibitor [40]. Other examples include FLT3/JAK2 dual inhibitor pacritinib [41] and FLT3/TOPK dual inhibitor HSD1169 [42] (**Figure 2**).

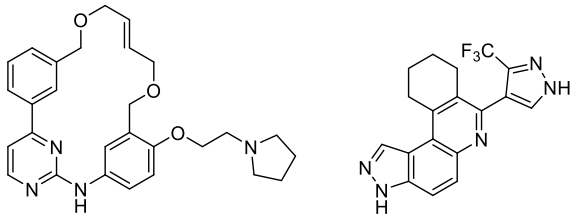

Figure 2. Chemical structures of reported dual FLT3 kinase inhibitors.

Several studies have investigated the role of tropomyosin receptor kinase A (TrKA) in AML [43–46]. TrKA is a receptor tyrosine kinase normally responsible for the survival and differentiation of neuronal tissue [47] and is additionally implicated in early hematopoiesis [48,49]. TrKA gene fusions and overexpression may contribute to AML growth and survival [45] and although the presence of TrKA fusions sensitized hematopoietic malignancies to TrKA inhibitors [46], the use of these kinase inhibitors as a single agent is not lethal in AML. Instead, combination therapy with inhibitors of related kinases or design of dual target inhibitors might be more efficient to tackle AML with TrKA fusions [45,50]. To date, many TrK kinase inhibitors were reported [51] and a few of these have received FDA approval including, multikinase inhibitor entrectinib [52], and selective pan-TrK inhibitor larotrectinib [53] (**Figure 3**). In addition, several approved or in clinical trials FLT3 inhibitors showed potent activity against TrKA including, gilteritinib (IC_{50} = 5 nM) [24], midostaurin (IC_{50} = 50 nM) [54], lestaurtinib (IC_{50} = 3.7 nM) [55], crenolanib [56], ponatinib (IC_{50} = 11.4 nM) [57], and rebastinib (IC_{50} = 11.4 nM) [58] (**Figure 3**).

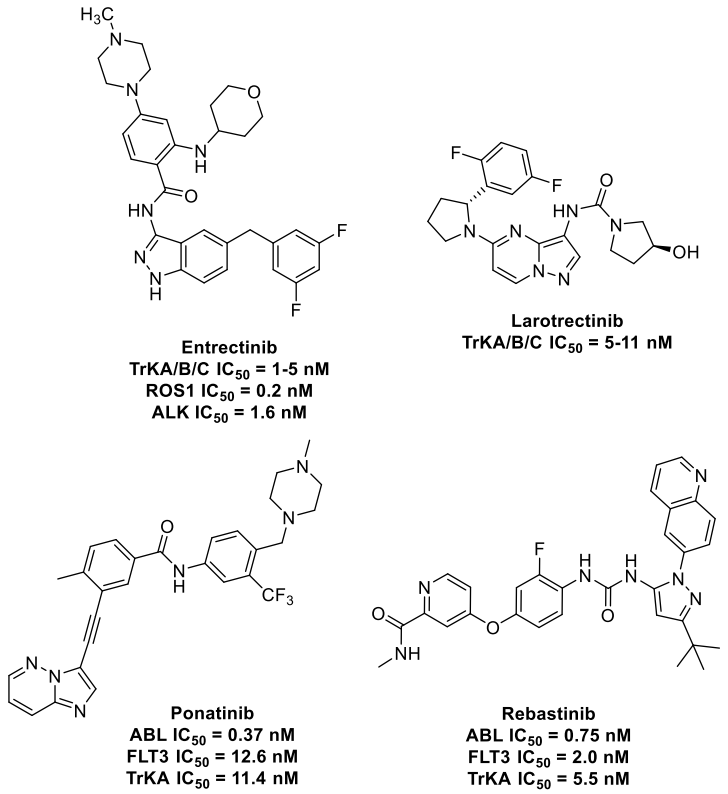

Figure 3. Chemical structures of reported TrKA inhibitors.

Considering the efficacy of FLT3 small molecule inhibitors as a validated AML therapy and the growing evidence of the beneficial use of dual kinase inhibitors to target AML heterogeneity, we herein report the discovery of a novel benzimidazole-based dual FLT3/TrKA kinase inhibitor as a potential therapeutic agent targeting AML.

2. Results and Discussion

2.1. Design Strategy

Quizartinib is a potent and selective FLT3 kinase inhibitor approved for use in Japan in 2019 for relapsed FLT3-ITD AML [59]. Although it showed potent nanomolar activity against FLT3 wild-type and FLT3-ITD mutations, being a type II kinase inhibitor, it lacked activity against FLT3-TKD mutations leading to its acquired resistance [60,61]. Additionally, despite quizartinib distinct kinase inhibition profile, it showed potent off-target inhibition of c-KIT [62], PDGFRα, PDGFRβ, RET, and CSF1R kinases [23]. Inhibition of c-KIT contributed to quizartinib "synthetic lethal toxicity" where concomitant inhibition of FLT3 and c-KIT led to myelosuppression [62,63]. In light of

quizartinib limitations and guided by ligand-based design, we developed a novel benzimidazole-based small molecule inhibitor (**4ACP**) with two potential objectives. First, to target FLT3-WT, FLT-ITD, and FLT3-D835Y (FLT3-TKD) mutations, consequently, targeting dependent AML cell lines. Second, to exhibit reduced activity against c-KIT kinase enzyme therefore limiting its toxicity. Our design strategy combined scaffold hopping of the hinge binder moiety of quizartinib, imidazo[2,1-*b*]thiazole, into a benzimidazole moiety, which was supported by the reported FLT3 activity of several benzimidazole-based derivatives designed as quizartinib analogues[64–66]and structure simplification by removing the 5-(*tert*-butyl)isoxazole part, which is likely responsible for quizartinib lack of activity against TKD mutations to yield **4ACP** as a potential FLT3 kinase inhibitor (**Figure 4**).

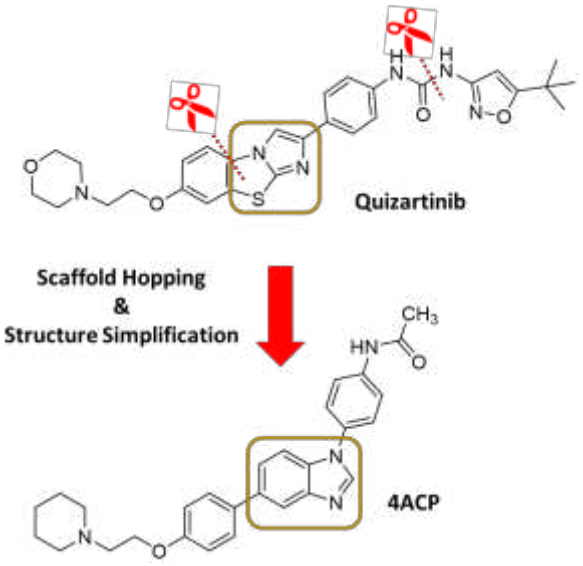

Figure 4. Design strategy for the benzimidazole-based kinase inhibitor, **4ACP**.

In order to validate our design, we docked the proposed compound, **4ACP**, into the ATP binding site of FLT3 enzyme using CDOCKER module of Discovery Studio® 2.5 software and compared its binding mode and interactions to that of quizartinib (**Figure 5A-5D**). Quizartinib binds to the inactive conformation of FLT3 enzyme (PDB code: 4XUF, DFG-out conformation) where the benzo(*d*)imidazo[2,1-*b*]thiazole fits in the hinge region and forms an essential hydrogen bond with Cys694 amino acid. The urea moiety extends into the allosteric channel forming two hydrogen bonds with Asp829 and Glu661 and ends with a 5-(tert-butyl)isoxazole that fits in the allosteric pocket of the inactive enzyme. Finally, the 7-(2-morpholinoethoxy) group

represents the solvent accessible group that does not affect the potency but rather improves the solubility [67]. In comparison, **4ACP**'s benzimidazole moiety occupied the hinge region and formed the essential hydrogen bond with Cys694, while the acetamido group extended slightly into the allosteric channel forming one hydrogen bond with Asp829 and leaving the allosteric pocket unoccupied. The 4-(2-(piperidin-1-yl)ethoxy) group acted as the solvent accessible group and formed an additional hydrogen bond with Cys695 amino acid. According to **4ACP** binding mode, it is anticipated that it would act as a type I kinase inhibitor and to further validate this proposition, we docked **4ACP** into the active conformation of FLT3 enzyme (PDB code: 6JQR, DFG-in conformation) (**Figure 5E**). As expected, **4ACP** could fit into the active site and maintain the essential interactions required for binding.

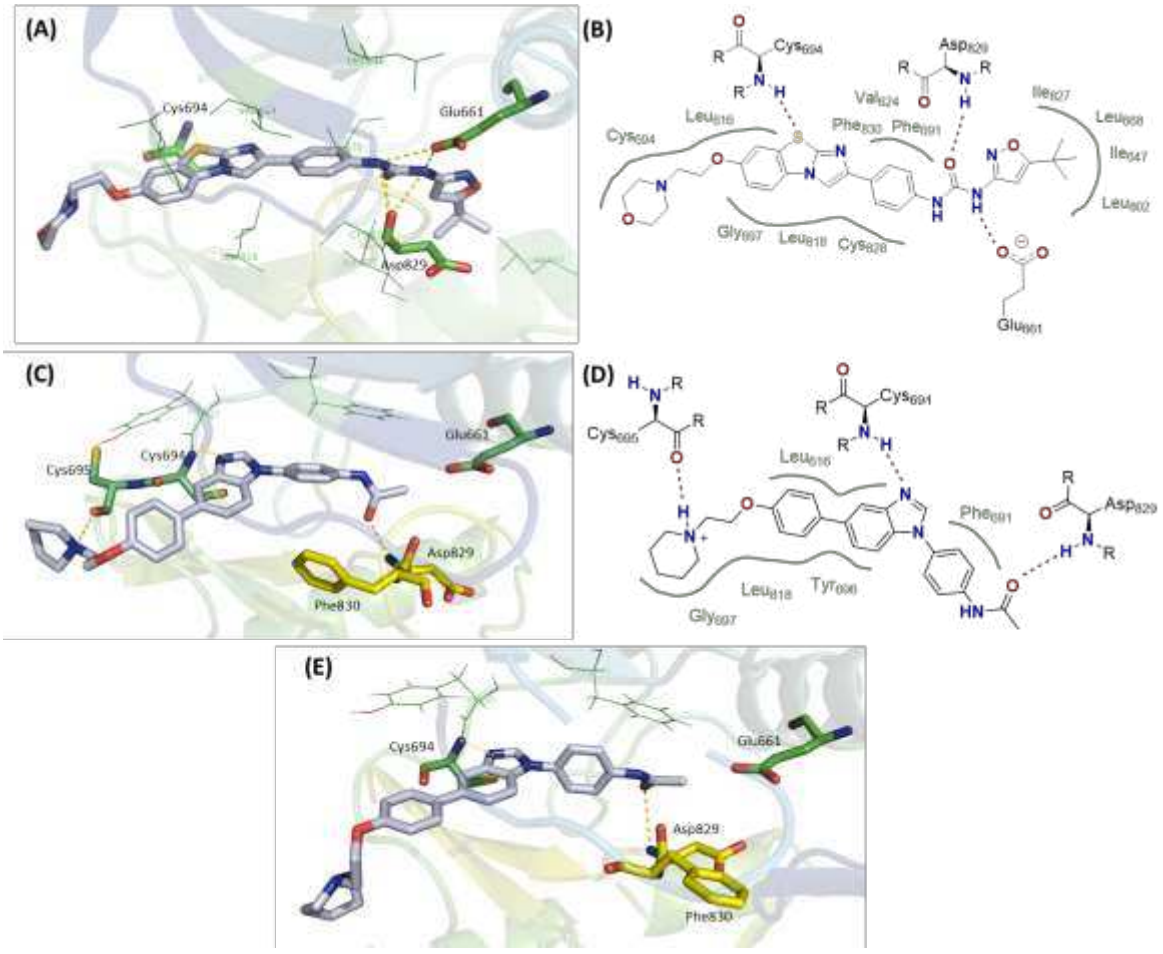

Figure 5. Quizartinib and 4ACP binding modes within FLT3 ATP binding site. (A), **(C)** 3D binding interactions of quizartininb and **4ACP** respectively within the ATP binding site of FLT3 enzyme (PDB code: 4XUF, DFG-out conformation). Quizartinib and **4ACP** are represented as sticks with white backbones, interacting amino acids are represented as sticks with green backbones, DFG motif is displayed as yellow sticks, and hydrogen bonds are

depicted in dotted lines. **(B)**, **(D)** 2D binding interactions of quizartinib and **4ACP** displaying the key amino acids involved in these interactions. **(E)** 3D binding interactions of **4ACP** within the ATP binding site of FLT3 enzyme (PDB code: 6JQR, DFG-in conformation).

2.2. Chemistry

The desired benzimidazole derivative (**4ACP**) was synthesized according to the previously reported procedures [68–71] as depicted in **Scheme 1**. Nucleophilic aromatic substitution of 5-bromo-2-fluoronitrobenzene (**1**) with 4-aminoacetanilide in DMF using K_2CO_3 yielded the desired *N*-(4-((4-bromo-2-nitrophenyl)amino)phenyl)acetamide (**2**) in 98% yield. Reduction of the nitro derivative (**2**) using $SnCl_2.2H_2O$ in EtOAc and subsequent cyclization by reflux in formic acid furnished the desired *N*-(4-(5-bromo-1*H*-benzimidazol-1-yl)phenyl)acetamide (**3**) in 93.7% yield. Suzuki coupling of the bromo derivative (**3**) with 4-hydroxyphenylboronic acid using Tetrakis(triphenylphosphine)palladium(0) and K_2CO_3 in dioxane and water yielded the desired *N*-(4-(5-(4-hydroxyphenyl)-1*H*-benzoimidazol-1-yl)phenyl)acetamide (**4**) in 50.5% yield. Alkylation of the hydroxy derivative (**4**) with 1-(2-Chloroethyl)piperidine hydrochloride in DMF using Cs_2CO_3 and few specks of KI gave the desired *N*-(4-(5-(4-(2-(piperidin-1-yl)ethoxy)phenyl)-1*H*-benzoimidazol-1-yl)phenyl)acetamide (**4ACP**) in 12% yield.

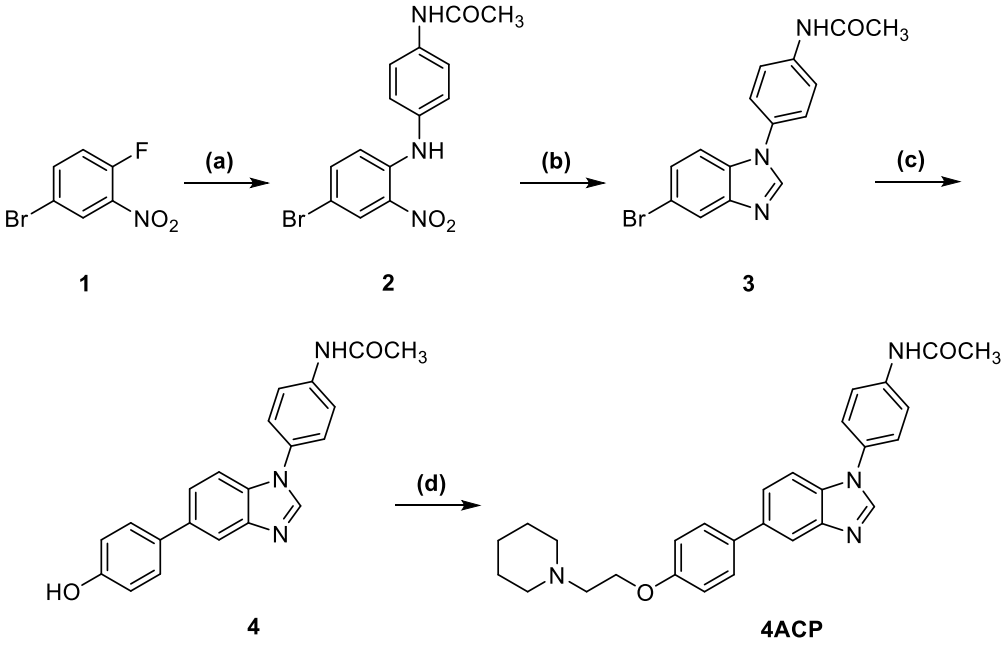

Scheme 1. Reagents and conditions: **(a)** 4-Aminoacetanilide, DMF, K_2CO_3, 80°C, 24 h, 98% yield; **(b) (1)** $SnCl_2.2H_2O$, EtOAc, reflux, 6 h, **(2)** HCOOH, reflux, 1 h, 93.7% yield; **(c)** 4-hydroxyphenylboronic acid, $Pd(PPh_3)_4$, K_2CO_3, dioxane, H_2O, reflux, 3 h, 50.5% yield; **(d)** 1-(2-Chloroethyl)piperidine hydrochloride, DMF, Cs_2CO_3, KI, 80°C, 24 h, 12% yield.

2.3. Biological activities

2.3.1. *In vitro* FLT3 kinase assays of 4ACP

As part of the mechanistic validation, we initially evaluated the activity of **4ACP** against wild-type FLT3, FLT3-ITD, and FLT-TKD (D835Y mutation) enzymes using *in vitro* kinase assay. **4ACP** showed potent activity against all three FLT3 forms (IC_{50} = 43.8, 97.2, and 92.5 nM respectively) (**Table 1**). Notably, **4ACP** showed equipotent activity against FLT3-ITD and FLT3-D835Y mutations as opposed to quizartinib that has negligible activity against FLT3-TKD mutations. Per our design, this can be ascribed to the possibility that **4ACP** acts as a type I kinase inhibitor, hence its ability to retain activity against FLT3-TKD mutations that confer resistance to type II kinase inhibitors [72,73].

Table 1. *In vitro* kinase inhibition and antiproliferative activities of **4ACP**.

Compound	Kinase enzymes IC_{50} (nM)[a]				Cell lines		
					IC_{50} (nM)[b]		GI_{50} (nM)
	FLT3	FLT3-ITD	FLT3-D835Y	TrKA	MOLM-13[c]	MV4-11[d]	KM12[e]
4ACP	43.8	97.2	92.5	23.6	38.8±10.7	54.9±4.1	358
Sorafenib	48.6	--	--	--	8.7±1.2	7.7±2.0	--
Quizartinib	--	--	--	--	1.10±0.036	0.62±0.098	--
Staurosporine	--	0.259	0.254	5.78	--	--	--

[a]The kinase inhibition assays were provided by ThermoFisher Scientific. All data were obtained by double testing.
[b]Median inhibitory concentration (IC_{50}) values are expressed as mean±SD and were based on the data obtained from triplicates of at least two independent experiments after 72 h treatment.
[c]AML-FLT3-ITD$^+$ (heterozygous).
[d]AML-FLT3-ITD$^+$ (homozygous).
[e]NCI-60 cell line screening data.

2.3.2. *In vitro* antiproliferative screening and TrKA enzyme inhibitory activity of 4ACP

In vitro enzyme assays identified FLT3 as a target selectively inhibited by **4ACP**. Hence, we sought to evaluate whether **4ACP** could selectively target FLT3-ITD positive AML cell lines. To this

end, we investigated the potential anti-leukemic activity of varying concentrations of **4ACP** on two FLT3-ITD harboring AML cell lines (MV4-11 and MOLM-13) using ATP Cell Titer Glo™ cell viability assay. Indeed, **4ACP** dramatically reduced the viability of MV4-11 and MOLM-13 in a concentration and time-dependent pattern (**Table 1** and **Figure 6**). Clonogenic assay also revealed that **4ACP** significantly impaired the clonogenic potential of FLT3-ITD positive MV4-11 and MOLM-13 cells (**Figure 7**).

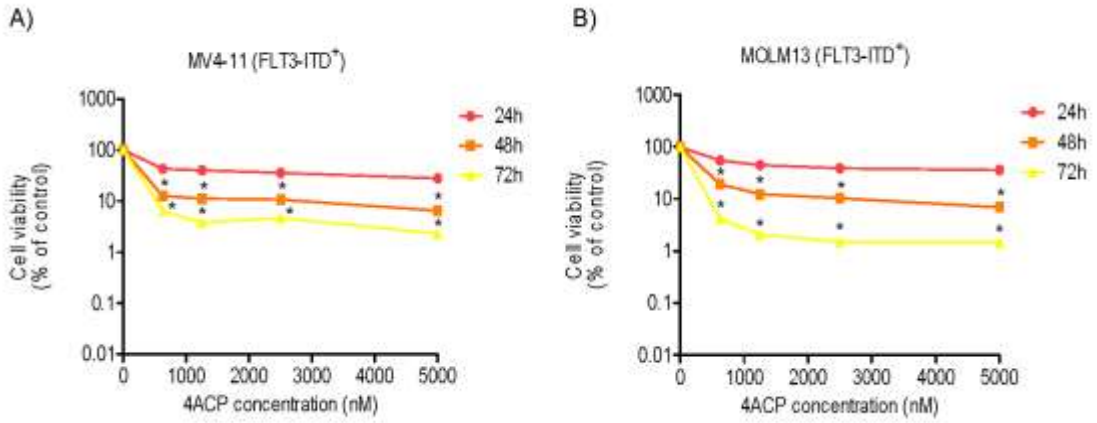

Figure 6. 4ACP significantly attenuates the viability of FLT3-ITD positive acute myeloid leukemia cells. (A), (B) Cell viability (cellular ATP%) normalized to vehicle-treated group of MV4-11 **(A)** and MOLM-13 **(B)** cells following their treatment with the indicated concentrations of **4ACP** for 24, 48 and 72h and assessed using ATP Cell Titer-Glo™ assay. *: Statistical significance as compared to the corresponding concentration of 24h **4ACP**-treated group assessed using Two-way analysis of variance (ANOVA) followed by Bonferroni post-test.

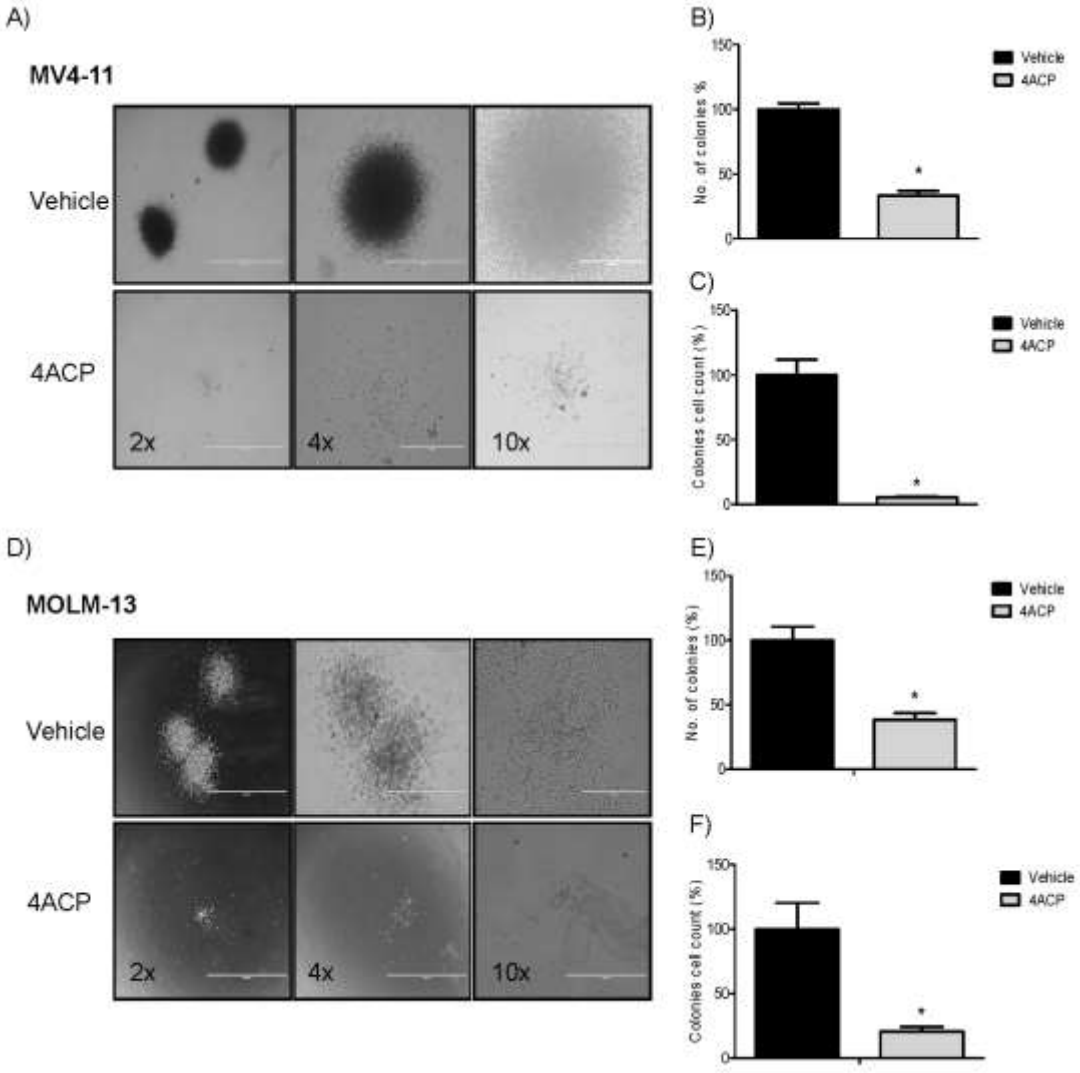

Figure 7. 4ACP evidently impairs the colony forming potential of FLT3-ITD positive acute myeloid leukemia cells. **(A)** Representative phase contrast images of the semisolid culture assay depicting MV4-11 colonies 14 days following their treated with either vehicle or **4ACP** (500 nM). **(B)**, **(C)** Percent of number of colonies **(B)** and colonies cell count **(C)** of MV4-11 cells treated with either vehicle or **4ACP** (500 nM) and cultured for 14 days in semisolid medium (n=3). *: Statistical significance as compared to vehicle-treated group assessed using Student's t-test. **(D)** Representative phase contrast images of the semisolid culture assay depicting MOLM-13 colonies 7 days following their treated with either vehicle or **4ACP** (500 nM). **(E)**, **(F)** Percent of number of colonies **(E)** and colonies cell count **(F)** of MOLM-13 cells treated with either vehicle or **4ACP** (500 nM) and cultured for 7 days in semisolid medium (n=3). *: Statistical significance as compared to vehicle-treated group assessed using Student's t-test.

Next, we questioned whether FLT3-ITD negative AML cell lines might be equally responsive to the anti-leukemic activity of **4ACP**. As a cellular selectivity control, we tested the anticancer activity of **4ACP** on two non FLT3 mutated AML cell lines which carry different types of mutations: THP-1 (MLL-AF9) and GDM-1 (CBL) [74,75]. **4ACP** did not elicit cytotoxic activity against

GDM-1 and THP-1 AML cell lines which do not carry FLT3-ITD mutation (**Figure 8** and **Supplementary data, S2, Figure S1A**). In contrast, GDM-1 AML cell line was vulnerable to the anticancer activity of sorafenib, a multikinase inhibitor (**Figure 8A**). This might be attributed to the inhibitory effects of sorafenib on other tyrosine kinase receptors as stem cell factor tyrosine kinase receptor (c-kit) which is overexpressed in GDM-1 cells [76]. Consistently, glioblastoma (U251) as well as clear cell renal cell carcinoma (Caki-1) cells were irresponsive to the anticancer doses of **4ACP** which potently inhibited the viability of FLT3-ITD harboring AML cell lines (**Supplementary data, S2, Figure S1B-1C**). Altogether, the present data indicate that **4ACP** preferentially targets FLT3-ITD positive AML cells.

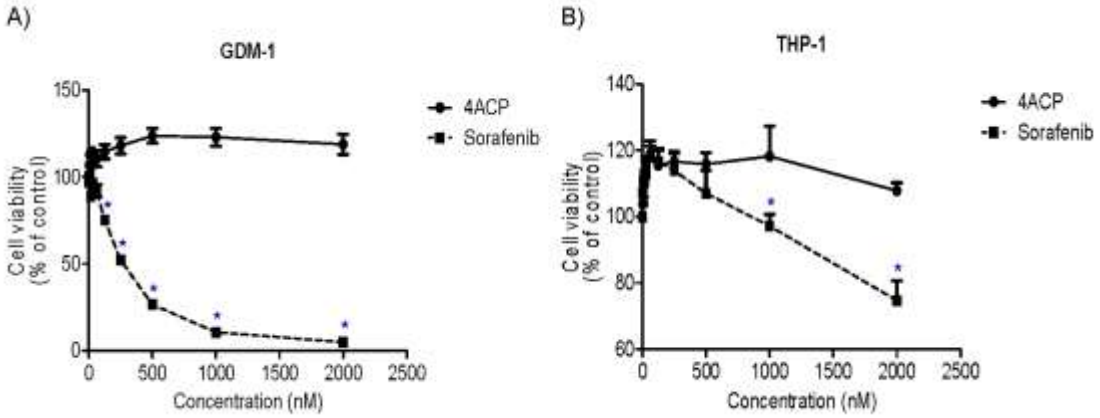

Figure 8. 4ACP does not affect the viability of FLT3-ITD negative acute myeloid leukemia cells. (A), **(B)** Cell viability (cellular ATP%) of GDM-1 **(A)** and THP-1 **(B)** cells 72h following their treatment with the indicated concentrations of **4ACP** or sorafenib normalized to vehicle-treated cells and assessed using ATP Cell Titer-Glo™ assay. *: Statistical significance as compared to the corresponding concentration of **4ACP**-treated group assessed using Two-way analysis of variance (ANOVA) followed by Bonferroni post-test.

Screening of **4ACP** using NCI-60 cell line panel demonstrated its ability to inhibit a limited number of cell lines at sub-micromolar concentrations (**Supplementary data, S3-S4**). Affected panel comprised, leukemia (K562 and SR), colon cancer (HCT-116, KM12, and SW620), and renal cancer (786-D) cell lines. Such discriminating antiproliferative activity of **4ACP** might indicate better selectivity and less off-target toxicity [77,78]. In particular, **4ACP** was most potent against colon cancer KM12 cell line (IC_{50} = 358 nM). Literature review revealed that KM12 cell line harbors an NTRK1 gene fusion encoding for a constitutively activated TrKA enzyme, rendering it sensitive to TrKA enzyme inhibitors [79]. Consequently, we proceeded with the *in vitro* assay of **4ACP** against

TrKA enzyme which demonstrated nanomolar activity (IC_{50} = 23.69 nM) (**Table 1**). Along with the previously conferred FLT3 kinase activity data, these results establish **4ACP** as a novel dual FLT3/TrKA small molecule inhibitor.

2.3.3. Western blot analysis of 4ACP effects in FLT3-ITD positive AML cells

FLT3-ITD activates extracellular regulated kinases 1/2 (ERK1/2) and mammalian target of rapamycin (mTOR) signaling which promote the survival and proliferation of AML cells [80]. To investigate whether **4ACP** could inhibit ERK1/2 and mTOR signaling downstream of FLT3-ITD, MV4-11 and MOLM-13 cells were treated with different concentrations (0, 10, 50 and 100 nM) of **4ACP** and lysates were harvested after 24 and 48h of treatment. Indeed, **4ACP** inhibited ERK1/2 and mTOR in FLT3-ITD positive AML cell lines in a dose-dependent manner (**Figure 9** and **Supplementary data, S5, Figure S2**). This is evidenced by prominent reduced phosphorylation and hence inactivation of ERK1/2 as well as p70 S6 kinase and ribosomal S6 (downstream target and readout of mTOR activity) in **4ACP**-treated FLT3-ITD positive AML cells as compared to vehicle-treated cells. Collectively, this data emphasize the inhibitory effect of **4ACP** on ERK1/2 and mTOR signaling downstream of FLT3-ITD in AML cells.

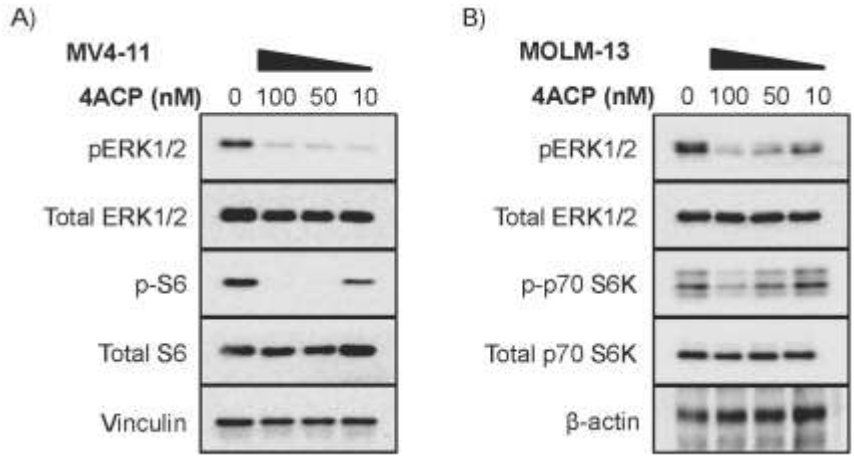

Figure 9. Immunoblot analysis of extracellular regulated kinases 1/2 (ERK1/2) and mammalian target of rapamycin (mTOR) signaling pathway in FLT3-ITD positive acute myeloid leukemia cells following their treatment with 4ACP. (A), **(B)** Western blot analysis of lysates obtained from MV4-11 **(A)** and MOLM-13 **(B)** cells 24h following their treatment with the indicated concentrations of **4ACP**. Vinculin was used as a loading control.

2.3.4. Cell cycle analysis of 4ACP effects in FLT3-ITD positive AML cells

FLT3 kinase inhibitors have been reported to induce G0/G1 cell cycle arrest [81]. Thereof, to investigate the effect of **4ACP** on cell cycle progression in FLT3-ITD positive AMLs, the DNA content of MV4-11 and MOLM-13 cells treated with varying concentrations (0, 10, 50 and 100 nM) of **4ACP** was assessed using flow cytometry. Consistently, **4ACP** remarkably induced a cell cycle arrest of MV4-11 and MOLM-13 cells at the G0/G1 phase (**Figure 10**).

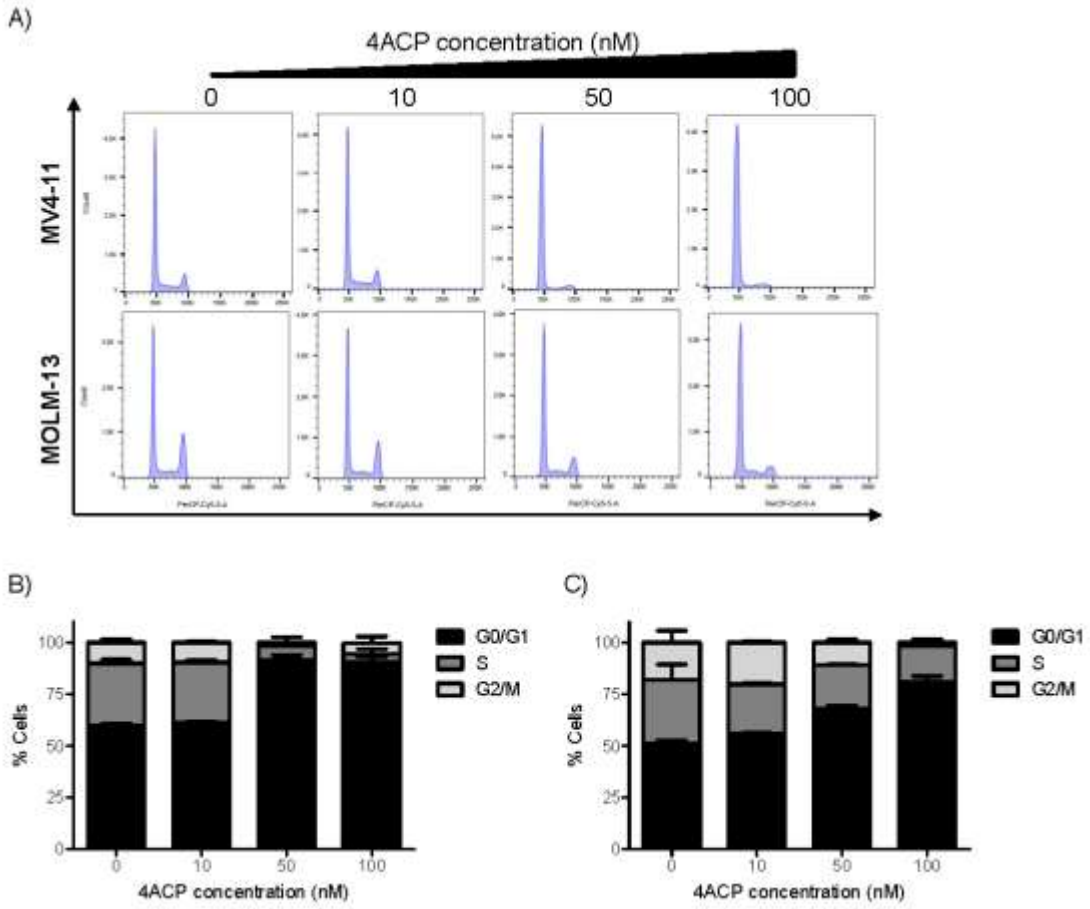

Figure 10. 4ACP triggers G0/G1 cell cycle arrest in FLT3-ITD positive acute myeloid leukemia cells. (A) Representative flow cytometric histograms depicting the cell cycle distribution of MV4-11 (upper panel) and MOLM-13 (lower panel) 72h following their treatment with the indicated concentrations of compound **4ACP** (0, 10, 50 and 100 nM). **(B)**, **(C)** Percentages of MV4-11 **(B)** and MOLM-13 **(C)** cells in G0/G1, S and G2/M phase 72h following their treatment with the indicated concentrations of **4ACP**.

Next, we explored whether **4ACP** could trigger cell death of FLT3-ITD positive AML cells using propidium iodide (PI), a fluorescent DNA-binding dye, which preferentially crosses the cell

membranes of apoptotic and necrotic cells. Indeed, flowcytometry analysis revealed that **4ACP** evidently triggered apoptotic and necrotic death of FLT3-ITD positive AML cells as evidenced by increased percent of PI positive cells in MV4-11 and MOLM-13 cells (**Figure 11**). Collectively, these findings indicate that **4ACP** induced G0/G1 cell cycle arrest as well as apoptotic and necrotic cell death of FLT3-ITD harboring AML cells.

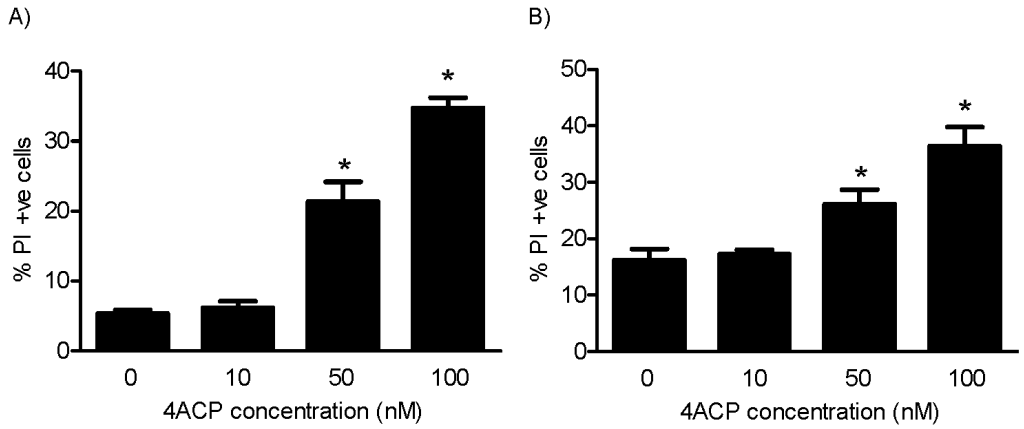

Figure 11. 4ACP induces apoptotic and necrotic cell death in FLT3-ITD positive acute myeloid leukemia cells. (A), **(B)** Percent of propidium iodide (PI) positive MV4-11 **(A)** and MOLM-13 **(B)** cells following their treatment with the indicated concentrations of **4ACP** for 72h using flow cytometry. *: Statistical significance as compared to vehicle-treated group assessed using One-way analysis of variance (ANOVA) followed by Dunnett test for post-hoc analysis.

2.3.5. *In vitro* cytotoxicity of 4ACP against normal BNL-hepatocytes and H9C2-cardiomyocytes

Multikinase inhibitors including FLT3 inhibitors have been associated with dose-limiting toxicities which result in dose reduction and/or interruption [74,82–84]. Hepatotoxicity as well as cardiotoxicity are among the toxicities associated with FLT3 inhibitors [82]. Thus, we sought to investigate the potential cytotoxic effect of **4ACP** on normal murine hepatocyte (BNL) and rat cardiomyoblast (H9c2) cells. **4ACP** did not elicit drastic cytotoxic effects on BNL and H9c2 cells (**Figure 12**). Collectively, these findings suggest that anticancer concentrations of **4ACP** might have a favorable safety profile on normal cells.

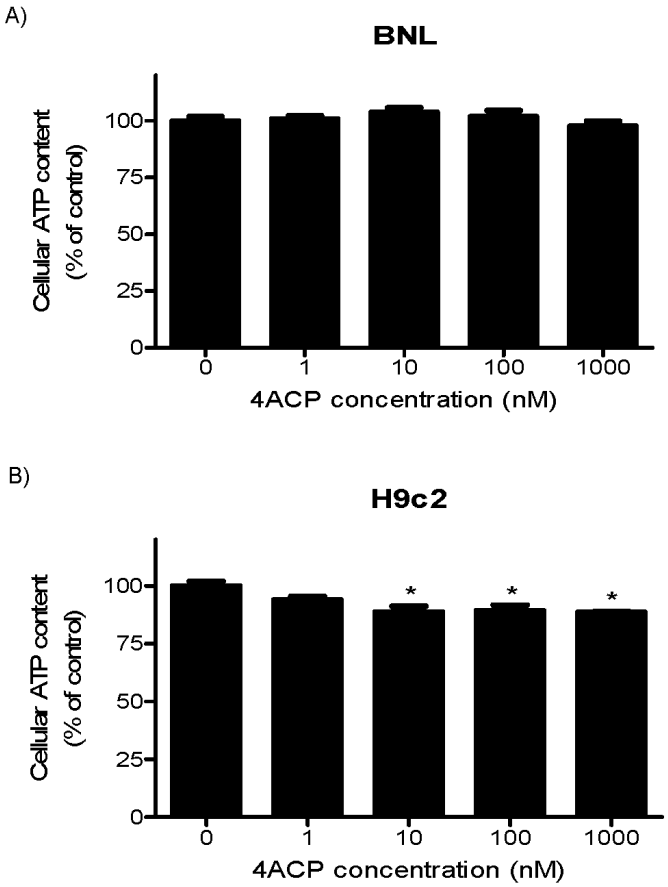

Figure 12. Anticancer concentrations of 4ACP do not dramatically compromise the viability of normal murine hepatocytes (BNL) and rat cardiomyoblasts (H9c2) cells. (A), **(B)** Cell viability (cellular ATP %) of murine hepatocyte (BNL) rat **(A)** and cardiomyoblast (H9c2) **(B)** cells 72h following their treatment with the indicated concentrations of **4ACP** normalized to vehicle-treated cells and assessed using ATP Cell Titer-Glo™ assay. *: Statistical significance as compared to vehicle-treated group assessed using One way analysis of variance (ANOVA) followed by Dunnett test for post-hoc analysis.

2.3.6. *In vitro* selectivity profiling of 4ACP against a panel of kinase enzymes

To further assess **4ACP** selectivity and to compare to other FLT3 inhibitors, we screened our compound against a panel of 17 kinases (**Table 2**). Our selection criteria was based on the off-target kinases potently inhibited by FLT3 inhibitors, quizartinib and sorafenib [23,85].

4ACP showed negligible to weak activity against FLT3-closely related kinases, FLT1, FLT4, PDGFRα, and PDGFRβ at 1 µM concentration. Advantageously, it showed more than 20-fold less potency against c-Kit kinase enzyme indicating its preferential selectivity towards FLT3 and lower potential to trigger synthetic lethal toxicity which induces myelosuppression side effect.

Assessment of our compound activity against other members of TrK family, TrKB and TrKC, showed that **4ACP** exhibited considerable activity against TrKA cognate partners which might designate **4ACP** as a pan-TrK inhibitor.

Table 2. *In vitro* kinase inhibition profile of **4ACP**.

Kinase	% Inhibition[a] at 1 μM	Kinase	% Inhibition[a] at 1 μM
ABL1	63	PDGFRα	41
CDK2/cyclin A	2	PDGFRβ	33
FGFR3	13	PIM1	9
FLT1 (VEGFR1)	13	PRKD2 (PKD2)	19
FLT4 (VEGFR3)	24	B-Raf	5
IGF1R	11	SRC	27
KDR (VEGFR2)	77	TrKB	70
c-KIT	36	TrKC	79
LCK	78		

[a]The kinase inhibition assays were provided by ThermoFisher Scientific. All data were obtained by double testing.

2.4. Molecular modeling

Molecular docking of **4ACP** into the ATP binding site of TrKA kinase enzyme (PDB code: 5KVT) using CDOCKER module of Discovery Studio® 2.5 software revealed a relatively similar binding mode to the bound ligand, entrectinib (**Figure 13**). The benzimidazole moiety of **4ACP** formed an essential hydrogen bond with the hinge region Met592 amino acid, while the *N*-(*p*-acetanilide) extended into the hydrophobic pocket and formed a hydrogen bond between the acetamido NH and Gly667 amino acid. The 4-(2-(piperidin-1-yl)ethoxy) group extended out of the active site into the solvent and formed an additional hydrogen bond with Leu516 amino acid.

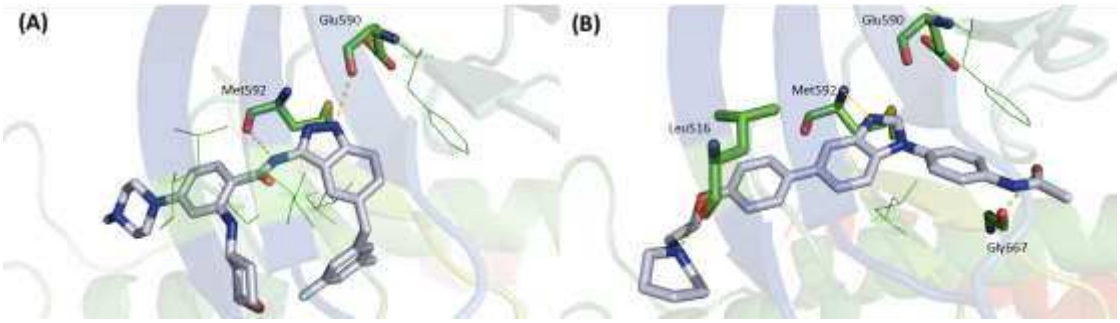

Figure 13. 4ACP binds to the ATP binding site of TrKA kinase enzyme in a similar mode to the reported inhibitor, entrictinib (PDB code: 5KVT). (A), (B) 3D binding poses and interactions of entrictinib and **4ACP** within the ATP binding site of TrKA enzyme. Both compounds are represented as sticks with white backbones, interacting amino acids are represented as sticks with green backnbones, and hydrogen bonds are depicted in dotted lines.

3. Conclusion

The aim of our study was to develop selective and potent analogues of quizartinib as potential FLT3 inhibitors targeting AML harboring FLT3 mutations. Guided by ligand-based design and structure simplification of quizartinib we developed a benzimidazole-based small molecule, **4ACP**, that exhibited nanomolar activity against wild-type FLT3, FLT3-ITD and FLT3-D835Y (FLT3-TKD) enzymes. Unlike quizartinib, **4ACP** displayed equipotent activity against both FLT3-ITD and FLT3-TKD mutations which might be attributable to the probability that **4ACP** acts as a type I kinase inhibitor. **4ACP** demonstrated selective antiproliferative activity against FLT3-ITD positive AML cell lines (MV4-11 and MOLM-13), while lacking activity against FLT3-ITD negative AML cell lines. NCI-60 cell line screening of **4ACP** showed a narrow panel of activity and deconvolution of **4ACP**'s potent activity against colon cancer KM12 cell line led to the identification of TrKA kinase enzyme as another target for **4ACP**, hence, designating our compound as a dual FLT3/TrKA kinase inhibitor. Recent studies correlate TrKA fusions and overexpression with AML growth and survival, and inhibition of TrKA enzyme along other AML-related kinases (i.e., FLT3 in this respect) might represent a more efficient approach to tackle hematopoietic malignancies.

Mechanistic studies demonstrated the ability of **4ACP** to inhibit ERK1/2 and mTOR signaling downstream of FLT3-ITD in AML cells. Furthermore, cell cycle analysis revealed that **4ACP** induced G0/G1 cell cycle arrest as well as apoptotic and necrotic cell death of FLT3-ITD positive AML cells. Moreover, **4ACP** produced no cytotoxic effects on normal murine hepatocyte and rat cardiomyoblast cells at concentrations exceeding 20-folds its IC_{50} values against FLT3-ITD

positive AML cells indicating a relatively safe profile. Additionally, **4ACP** had diminished activity against c-Kit enzyme implying a likely lower incidence of myelosuppression.

Collectively, these data corroborate the therapeutic potential of **4ACP** as a dual FLT3/TrKA inhibitor targeting AML and further assessment and SAR investigation are warranted.

4. Experimental

4.1. Chemistry

Chemicals and solvents were purchased from Sigma-Aldrich (Germany) and Alfa Aesar (Germany) and were used as such without further purification. Reactions were followed using analytical thin layer chromatography (TLC), performed on Aluminum silica gel 60 F_{254} TLC plates, purchased from Merck, with visualization under UV light (254 nm). ^{1}HNMR spectra were determined on a Bruker Avance III HD FT NMR spectrometer operating at 9.4 T (400 MHz) or a two-channel Bruker AV-NEO NMR spectrometer operating at 11.7 T (500 MHz) in δ scale (ppm) and *J* (Hz) and referred to the deuterated solvent peak (DMSO-d_6 δ = 2.5 ppm). ^{13}CNMR spectra were determined on the two-channel Bruker AV-NEO NMR spectrometer at 126 MHz and referred to the solvent peak (DMSO-d_6 δ = 39.52 ppm). All NMR datasets were acquired at 298 K unless otherwise stated. High resolution mass spectrometry (HRMS) was carried out using a Bruker MaXis Impact Time of Flight spectrophotometer, using electrospray ionization (ES +). The purity of the final compounds was assessed by HPLC on an Agilent 1290 Infinity Series equipped with a UV detector and a C_{18} reverse phase column eluting with an MeCN – water gradient (5-95%) and 0.1% TFA over 5 mins at a flow rate of 0.5 mL min^{-1}

4.1.1. Synthetic procedures for 4ACP

The desired benzimidazole derivative (**4ACP**) was synthesized according to the previously reported procedures [68–71] and is illustrated as follows.

Step a: To a solution of 5-bromo-2-fluoronitrobenzene (**1**) (5.00 g, 22.7 mmol, 1.00 equiv) in DMF (20 ml) was added 4-aminoacetanilide (3.75 g, 25.0 mmol, 1.10 equiv) and K_2CO_3 (3.80 g, 27.5 mmol, 1.20 equiv) and the reaction mixture was heated at 80^{o}C for 24 h. Upon completion of the reaction as indicated by TLC, the mixture was cooled, poured into ice/water, and stirred

for 1 h. The resulting precipitate was filtered, washed with water, and dried to give the desired *N*-(4-((4-bromo-2-nitrophenyl)amino)phenyl)acetamide (**2**) as deep reddish solid in 98% yield. **^{1}H NMR (400 MHz, DMSO-d_6)**: δ, ppm 10.03 (s, 1H), 9.43 (s, 1H), 8.21 (s, 1H), 7.72 – 7.52 (m, 3H), 7.25 (d, *J* = 7.3 Hz, 2H), 7.00 (d, *J* = 8.6 Hz, 1H), 2.06 (s, 3H).

Step b: To a solution of *N*-(4-((4-bromo-2-nitrophenyl)amino)phenyl)acetamide (**2**) (7.70 g, 22.0 mmol, 1.00 equiv) in EtOAc (150 ml) was added $SnCl_2.2H_2O$ (24.8 g, 110 mmol, 5.00 equiv) and the reaction mixture was refluxed for 6 h. Upon completion of the reaction as indicated by TLC, the mixture was cooled, washed with sodium carbonate solution (10%), separated, dried over anhydrous Na_2SO_4 and evaporated to give the amine intermediate, *N*-(4-((2-amino-4-bromophenyl)amino)phenyl)acetamide as red residue. To this residue was added formic acid (20 ml) and the reaction mixture was refluxed for 1 h. Upon completion of the reaction as indicated by TLC, the mixture was cooled, neutralized with cold sodium carbonate solution (10%), and stirred for 1 h. The resulting solid was filtered, washed with water, diethyl ether and dried to afford the desired *N*-(4-(5-bromo-1*H*-benzimidazol-1-yl)phenyl)acetamide (**3**) as light violet solid in 93.7% yield. **^{1}H NMR (400 MHz, DMSO-d_6)**: δ, ppm 10.22 (s, 1H), 8.57 (s, 1H), 7.98 (s, 1H), 7.82 (d, *J* = 8.6 Hz, 2H), 7.60 (d, *J* = 8.7 Hz, 2H), 7.55 (d, *J* = 8.6 Hz, 1H), 7.46 (d, *J* = 8.5 Hz, 1H), 2.10 (s, 3H).

Step c: A solution of *N*-(4-(5-bromo-1*H*-benzimidazol-1-yl)phenyl)acetamide (**3**) (500 mg, 1.51 mmol, 1.00 equiv) and 4-Hydroxybenzeneboronic acid (418 mg, 3.03 mmol, 2.00 equiv) in dioxane/water (4:1, 24 ml) was purged with nitrogen for 5 min then $Pd(PPh_3)_4$ (35 mg, 0.03 mmol, 0.02 equiv) and K_2CO_3 (626 mg, 4.53 mmol, 3.00 equiv) were added and the reaction was refluxed under nitrogen for 3 hr. Upon completion of the reaction as indicated by TLC, the mixture was cooled, filtered using celite, evaporated, and the resulting residue was extracted with ethyl acetate. The organic layer was dried over anhydrous Na_2SO_4, evaporated, and the resulting residue was purified by flash chromatography (DCM/MeOH 9.5:0.5) to yield the desired *N*-(4-(5-(4-hydroxyphenyl)-1*H*-benzoimidazol-1-yl)phenyl)acetamide (**4**) as greyish white solid in 50.5% yield. **^{1}H NMR (400 MHz, DMSO-d_6)**: δ, ppm 10.21 (s, 1H), 9.51 (s, 1H), 8.51 (s, 1H), 7.92 (s, 1H), 7.83 (d, *J* = 8.5 Hz, 2H), 7.65 – 7.58 (m, 3H), 7.55 (d, *J* = 8.4 Hz, 3H), 6.87 (d, *J* = 8.4 Hz, 2H), 2.11 (s, 3H).

Step d: To a solution of *N*-(4-(5-(4-hydroxyphenyl)-1*H*-benzoimidazol-1-yl)phenyl) acetamide (**4**) (190 mg, 0.55 mmol, 1.00 equiv) and 1-(2-Chloroethyl)piperidine hydrochloride (204 mg, 1.10 mmol, 2.00 equiv) in DMF (5 ml) was added Cs_2CO_3 (721 mg, 2.21 mmol, 4.00 equiv) and few specks of KI and the reaction mixture was heated at 80^{o}C for 24 h. Upon completion of the reaction as indicated by TLC, the mixture was cooled, poured into ice/water, and stirred for 1 h. The resulting precipitate was filtered, washed with water, dried, and purified by flash chromatography (DCM/MeOH 9:1) to furnish the desired product, *N*-(4-(5-(4-(2-(piperidin-1-yl)ethoxy)phenyl)-1*H*-benzoimidazol-1-yl)phenyl)acetamide (**4ACP**) as off-white solid in 12% yield. **^{1}H NMR (501 MHz, DMSO-d_6)**: δ, ppm 10.27 (s, 1H), 8.53 (s, 1H), 7.97 (d, *J* = 1.1 Hz, 1H), 7.85 (d, *J* = 8.9 Hz, 2H), 7.66 (d, *J* = 8.8 Hz, 2H), 7.63 (d, *J* = 8.8 Hz, 3H), 7.58 (q, *J* = 3.4 Hz, 1H), 7.05 (d, *J* = 8.7 Hz, 2H), 4.18 (s, 2H), 2.81 (s, 2H), 2.58 (s, 4H), 2.11 (s, 3H), 1.56 (s, 4H), 1.43 (s, 2H). **^{13}C NMR (126 MHz, DMSO-d_6)**: δ, ppm 169.05, 158.10, 144.91, 144.32, 139.35, 135.21, 133.72, 132.89, 131.14, 128.46, 124.59, 122.80, 120.55, 117.66, 115.47, 111.41, 65.66, 57.40, 54.57, 25.52, 24.52, 23.97. **HRMS exact mass of $C_{28}H_{31}N_4O_2$ $(M+H)^+$:** 455.2442 amu; **found:** 455.2438 amu. **HPLC purity:** 95%, **HPLC t_R:** 1.68 min.

4.2. Biological activities

4.2.1. Reagents and antibodies

ROCHE Complete™ EDTA-free Protease Inhibitor Cocktail (Catalog.No.11836170001) was purchased from Sigma Aldrich. Bio-Rad DC™ Protein Assay (Catalog.No.500-0114) was purchased from Bio-Rad. Primary antibodies p-p70 S6 kinase (T389) (9234), total p70 S6K, pS6 (S235/236) (2211), total S6 (54D2), p-ERK1/2 (T202/Y204) (4370) and total ERK (4695) were purchased from Cell Signaling Technology. Anti-vinculin and anti-β-actin were purchased from Sigma Aldrich. Sorafenib and quizartinib were obtained from Selleckchem.

4.2.2. Human cancer and normal cell lines and cell culture

Patient-derived AML cell lines; MOLM-13, MV4-11 and GDM-1 were obtained from DSMZ. THP-1 was obtained from ATCC. MV4-11 and THP-1 cells were cultured in RPMI-1640 media supplemented with 2mM L-glutamine, 10% FBS and 1% penicillin-streptomycin. MOLM-13 and

GDM-1 cells were cultured in RPMI-1640 media supplemented with 20% FBS, 2mM L-glutamine and 1% penicillin-streptomycin. Normal murine hepatocyte (BNL) and rat cardiomyoblast (H9c2) cell lines were cultured in DMEM media supplemented with 10% FBS, 2mM L-glutamine and 1% penicillin-streptomycin. Cells were maintained in a humidified tissue culture incubator at 37ºC with 5% CO_2.

4.2.3. Cell viability assay

To determine the effect of **4ACP** on their viability, MOLM-13, MV4-11, GDM-1 and THP-1 cells were treated with varying concentrations of 4ACP for the indicated time points. Two FLT3 inhibitors sorafenib (first generation) and quizartinib (second generation) were also tested as reference FLT3 inhibitors. Cell viability was determined using a Cell Titer-Glo™ Luminescent Cell Viability assay (Promega Corporation, USA) which quantifies cellular ATP levels as an indicator of metabolically active cells [86]. Luminescence was assessed using Glomax™ Multi-Detection System (Promega Corporation, USA).

3.2.4. Clonogenic assay

MOLM-13 and MV4-11 cells were treated as indicated and cultured in MethoCult H4435 Enriched (StemCell Technologies, Vancouver, BC) and colonies were then counted as previously described [87].

3.2.5. Cell cycle analysis

Cell cycle analysis was carried out using propidium iodide staining and performed using FACS Celesta as previously described [88,89]. Analysis of cell cycle distribution pattern was performed using FlowJo software.

3.2.6. Quantification of cell death

After the treatment of MOLM-13 and MV4-11 cells as indicated, cells were washed in PBS (pH 7.2), and then stained with propidium iodide. Cell fluorescence was then measured using a

flow cytometer (FACSCalibur; Becton Dickinson, CA) and analyzed using FlowJo software as previously described [86].

3.2.7. Immunoblot analysis

Twenty-four and forty-eight hours following the treatment of MV4-11 and MOLM-13 cells with the indicated concentrations of **4ACP**, cells were harvested and lysed in HEPES lysis buffer comprising ROCHE Complete™ EDTA-free Protease Inhibitor Cocktail and western blot analysis was performed as previously described [90].

3.2.8. Statistical Analysis

Analysis of data was performed using GraphPad InStat (version 2) as follows; data are presented as mean ± standard deviation (SD). Unless otherwise indicated, Student's t-test was exploited to compare two different treatment groups. One way analysis of variance (ANOVA) followed by Dunnett test for *post-hoc* analysis was used for multiple comparisons for more than two treatment groups. To compare more than two treatment/timepoint groups with multiple concentrations each, Two-way ANOVA followed by Bonferroni test for post-test was exploited. Statistical significance was acceptable at P value < 0.05. Graphs were presented using GraphPad Prism software program (GraphPad software incorporated, version 5).

4.3. Molecular modeling

Molecular docking of **4ACP** was performed using Discovery Studio® CDOCKER protocol (version 2.5, Accelrys, Inc., San Diego, CA). The X-ray crystal structures of FLT3 (inactive and active conformations) and TrKA enzymes were obtained from PDB server (PDB codes: 4XUF, 6JQR, and 5KVT respectively). The protein structures were prepared according to the standard protein preparation procedure integrated in Accelry's Discovery Studio 2.5, which involved adding hydrogen atoms, completing the missing loops, and assigning force field parameters. CHARMM force field was used for simulation studies and then the protein structures were minimized using 1000 iterations of steepest descent minimization algorithm. The ligand was drawn using the sketching tools of Accelry's Discovery Studio and it was prepared for docking by adding hydrogen

atoms and partial charges using the Momany-Rone method. For docking, the CDOCKER protocol was used. The binding site was defined by the residues within 10 Å distance from the co-crystallized ligand. The default values of CDOCKER were used. Ten different docking solutions were generated and visually inspected for selection of the best binding mode. The results were viewed using PyMOL software (v2.3, https://pymol.org/2/).

Acknowledgment

AKA has been awarded a fellowship from Fondazione IEO-CCM. SNM has been awarded a PhD scholarship at University of Leeds funded by the Newton-Mosharafa Fund jointly offered by the British Council and the Ministry of Higher Education of the Arab Republic of Egypt. We thank Dr Jeanine Williams (School of Chemistry, University of Leeds) for conducting the HPLC purity determination assays. We thank Dr. Ciro Mercurio (Drug Discovery Unit, IFOM) for the kind provision of quizartinib.

Funding

This research did not receive any specific grant from funding agencies in the public, commercial, or not-for-profit sectors.

Conflicts of interest

The authors declare no competing financial interest.

Appendix A. Supplementary material

Supplementary data to this article can be found online at https://doi.org/xxxxxxx.

Abbreviations

FLT3, FMS-like tyrosine kinase 3; TrKA, Tropomyosin receptor kinase A; AML, Acute myeloid leukemia; ITD, Internal tandem duplication; TKD, Tyrosine kinase domain; ERK1/2, Extracellular signal-regulated protein kinases 1/2; mTOR, Mammalian target of rapamycin; c-Kit, Stem cell factor tyrosine kinase receptor; WT, Wild-type; DFG, Asp-Phe-Gly; TKIs, Tyrosine kinase inhibitors; SYK, Spleen tyrosine kinase; PDGFR, Platelet-derived growth factor receptor; AXL,

Tyrosine protein kinase receptor UFO; JAK2, Janus kinase 2; TOPK, T-LAK cell-originated protein kinase; RET, Rearranged during Transfection tyrosine kinase; CSF1R, Colony stimulating factor 1 receptor; PI, Propidium iodide; Abl1, Abelson tyrosine protein kinase 1; CDK2/cyclin A, Cyclin dependent kinase 2/cyclin A; FGFR3, Fibroblast growth factor receptor 3; VEGFR, Vascular endothelial growth factor receptor; IGF1R, Insulin-like growth factor 1; LCK, Lymphocyte-specific protein tyrosine kinase, PIM1, Proviral Integration site for Moloney leukemia virus 1; PRKD2, Protein Kinase D2; B-Raf, serine/threonine-protein kinase; SRC, Proto-oncogene tyrosine-protein kinase Src.

References

1. Short NJ, Rytting ME, Cortes JE. Acute myeloid leukaemia. *Lancet*. 2018;392(10147):593-606. doi:10.1016/S0140-6736(18)31041-9
2. Dombret H, Gardin C. An update of current treatments for adult acute myeloid leukemia. *Blood*. 2016;127(1):53-61. doi:10.1182/blood-2015-08-604520
3. Siegel RL, Miller KD, Jemal A. Cancer statistics, 2020. *CA Cancer J Clin*. 2020;70(1):7-30. doi:10.3322/caac.21590
4. De Kouchkovsky I, Abdul-Hay M. 'Acute myeloid leukemia: A comprehensive review and 2016 update.' *Blood Cancer J*. 2016;6(7):441. doi:10.1038/bcj.2016.50
5. Kantarjian H, Kadia T, DiNardo C, et al. Acute myeloid leukemia: current progress and future directions. *Blood Cancer J*. 2021;11(2):41. doi:10.1038/s41408-021-00425-3
6. Richard-Carpentier G, DiNardo CD. Single-agent and combination biologics in acute myeloid leukemia. *Hematol (United States)*. 2019;2019(1):548-556. doi:10.1182/hematology.2019000059
7. Short NJ, Konopleva M, Kadia TM, et al. Advances in the treatment of acute myeloid leukemia: New drugs and new challenges. *Cancer Discov*. 2020;10(4):506-525. doi:10.1158/2159-8290.CD-19-1011
8. Gary Gilliland D, Griffin JD. The roles of FLT3 in hematopoiesis and leukemia. *Blood*. 2002;100(5):1532-1542. doi:10.1182/blood-2002-02-0492
9. Grafone T, Palmisano M, Nicci C, Storti S. An overview on the role of FLT3-tyrosine kinase

receptor in acute myeloid leukemia: Biology and treatment. *Oncol Rev*. 2012;6(1):64-74. doi:10.4081/oncol.2012.e8

10. Cancer Genome Atlas Research Network, Ley TJ, Miller C, et al. Genomic and Epigenomic Landscapes of Adult De Novo Acute Myeloid Leukemia. *N Engl J Med*. 2013;368(22):2059-2074. doi:10.1056/nejmoa1301689
11. Papaemmanuil E, Gerstung M, Bullinger L, et al. Genomic Classification and Prognosis in Acute Myeloid Leukemia. *N Engl J Med*. 2016;374(23):2209-2221. doi:10.1056/nejmoa1516192
12. Yamamoto Y, Kiyoi H, Nakano Y, et al. Activating mutation of D835 within the activation loop of FLT3 in human hematologic malignancies. *Blood*. 2001;97(8):2434-2439. doi:10.1182/blood.V97.8.2434
13. Kiyoi H, Kawashima N, Ishikawa Y. FLT3 mutations in acute myeloid leukemia: Therapeutic paradigm beyond inhibitor development. *Cancer Sci*. 2020;111(2):312-322. doi:10.1111/cas.14274
14. Short NJ, Kantarjian H, Ravandi F, Daver N. Emerging treatment paradigms with FLT3 inhibitors in acute myeloid leukemia. *Ther Adv Hematol*. 2019;10:2040620719827310. doi:10.1177/2040620719827310
15. Lai C, Doucette K, Norsworthy K. Recent drug approvals for acute myeloid leukemia. *J Hematol Oncol*. 2019;12(1). doi:10.1186/s13045-019-0774-x
16. Yu J, Jiang PYZ, Sun H, et al. Advances in targeted therapy for acute myeloid leukemia. *Biomark Res*. 2020;8(1):1-11. doi:10.1186/s40364-020-00196-2
17. Orgueira AM, Pérez LB, Torre AM, et al. FLT3 inhibitors in the treatment of acute myeloid leukemia: Current status and future perspectives. *Minerva Med*. 2020;111(5):427-442. doi:10.23736/S0026-4806.20.06989-X
18. O'Farrell AM, Abrams TJ, Yuen HA, et al. SU11248 is a novel FLT3 tyrosine kinase inhibitor with potent activity in vitro and in vivo. *Blood*. 2003;101(9):3597-3605. doi:10.1182/blood-2002-07-2307
19. Weisberg E, Boulton C, Kelly LM, et al. Inhibition of mutant FLT3 receptors in leukemia cells by the small molecule tyrosine kinase inhibitor PKC412. *Cancer Cell*. 2002;1(5):433-

443. doi:10.1016/S1535-6108(02)00069-7

20. Levis M, Allebach J, Tse KF, et al. A FLT3-targeted tyrosine kinase inhibitor is cytotoxic to leukemia cells in vitro and in vivo. *Blood*. 2002;99(11):3885-3891. doi:10.1182/blood.V99.11.3885
21. Kelly LM, Yu JC, Boulton CL, et al. CT53518, a novel selective FLT3 antagonist for the treatment of acute myelogenous leukemia (AML). *Cancer Cell*. 2002;1(5):421-432. doi:10.1016/S1535-6108(02)00070-3
22. Auclair D, Miller D, Yatsula V, et al. Antitumor activity of sorafenib in FLT3-driven leukemic cells. *Leukemia*. 2007;21(3):439-445. doi:10.1038/sj.leu.2404508
23. Zarrinkar PP, Gunawardane RN, Cramer MD, et al. AC220 is a uniquely potent and selective inhibitor of FLT3 for the treatment of acute myeloid leukemia (AML). *Blood*. 2009;114(14):2984-2992. doi:10.1182/blood-2009-05-222034
24. Mori M, Kaneko N, Ueno Y, et al. Gilteritinib, a FLT3/AXL inhibitor, shows antileukemic activity in mouse models of FLT3 mutated acute myeloid leukemia. *Invest New Drugs*. 2017;35(5):556-565. doi:10.1007/s10637-017-0470-z
25. Galanis A, Ma H, Rajkhowa T, et al. Crenolanib is a potent inhibitor of flt3 with activity against resistance-Conferring point mutants. *Blood*. 2014;123(1):94-100. doi:10.1182/blood-2013-10-529313
26. Hassanein M, Almahayni MH, Ahmed SO, Gaballa S, El Fakih R. FLT3 Inhibitors for Treating Acute Myeloid Leukemia. *Clin Lymphoma, Myeloma Leuk*. 2016;16(10):543-549. doi:10.1016/j.clml.2016.06.002
27. Zhong Y, Qiu RZ, Sun SL, et al. Small-Molecule Fms-like Tyrosine Kinase 3 Inhibitors: An Attractive and Efficient Method for the Treatment of Acute Myeloid Leukemia. *J Med Chem*. 2020;63(21):12403-12428. doi:10.1021/acs.jmedchem.0c00696
28. Tong L, Li X, Hu Y, Liu T. Recent advances in FLT3 inhibitors for acute myeloid leukemia. *Future Med Chem*. 2020;12(10):961-981. doi:10.4155/fmc-2019-0365
29. Wang Z, Cai J, Cheng J, et al. FLT3 Inhibitors in Acute Myeloid Leukemia: Challenges and Recent Developments in Overcoming Resistance. *J Med Chem*. 2021;64(6):2878-2900. doi:10.1021/acs.jmedchem.0c01851

30. Lam SSY, Leung AYH. Overcoming resistance to flt3 inhibitors in the treatment of flt3-mutated aml. *Int J Mol Sci*. 2020;21(4). doi:10.3390/ijms21041537
31. Zhou J, Chng WJ. Resistance to FLT3 inhibitors in acute myeloid leukemia: Molecular mechanisms and resensitizing strategies. *World J Clin Oncol*. 2018;9(5):90-97. doi:10.5306/wjco.v9.i5.90
32. Scholl S, Fleischmann M, Schnetzke U, Heidel FH. Molecular Mechanisms of Resistance to FLT3 Inhibitors in Acute Myeloid Leukemia: Ongoing Challenges and Future Treatments. *Cells*. 2020;9(11). doi:10.3390/cells9112493
33. Yilmaz M, Alfayez M, Dinardo CD, et al. Outcomes with sequential FLT3-inhibitor-based therapies in patients with AML. *J Hematol Oncol*. 2020;13(1):132. doi:10.1186/s13045-020-00964-5
34. Maiti A, DiNardo CD, Daver NG, et al. Triplet therapy with venetoclax, FLT3 inhibitor and decitabine for FLT3-mutated acute myeloid leukemia. *Blood Cancer J*. 2021;11(2):25. doi:10.1038/s41408-021-00410-w
35. Xu B, Zhao Y, Wang X, Gong P, Ge W. MZH29 is a novel potent inhibitor that overcomes drug resistance FLT3 mutations in acute myeloid leukemia. *Leukemia*. 2017;31(4):913-921. doi:10.1038/leu.2016.297
36. Smith CC, Levis MJ, Frankfurt O, et al. A phase 1/2 study of the oral FLT3 inhibitor pexidartinib in relapsed/ refractory FLT3-ITD–mutant acute myeloid leukemia. *Blood Adv*. 2020;4(8):1711-1721. doi:10.1182/bloodadvances.2020001449
37. Yamaura T, Nakatani T, Uda K, et al. A novel irreversible FLT3 inhibitor, FF-10101, shows excellent efficacy against AML cells with FLT3 mutations. *Blood*. 2018;131(4):426-438. doi:10.1182/blood-2017-05-786657
38. Hospital MA, Green AS, Maciel TT, et al. FLT3 inhibitors: Clinical potential in acute myeloid leukemia. *Onco Targets Ther*. 2017;10:607-615. doi:10.2147/OTT.S103790
39. Mologni L, Marzaro G, Redaelli S, Zambon A. Dual kinase targeting in leukemia. *Cancers (Basel)*. 2021;13(1):1-26. doi:10.3390/CANCERS13010119
40. Yuan T, Qi B, Jiang Z, et al. Dual FLT3 inhibitors: Against the drug resistance of acute myeloid leukemia in recent decade. *Eur J Med Chem*. 2019;178:468-483.

doi:10.1016/j.ejmech.2019.06.002

41. Hart S, Goh KC, Novotny-Diermayr V, et al. Pacritinib (SB1518), a JAK2/FLT3 inhibitor for the treatment of acute myeloid leukemia. *Blood Cancer J*. 2011;1(11):e44. doi:10.1038/bcj.2011.43
42. Dayal N, Opoku-Temeng C, Hernandez DE, et al. Dual FLT3/TOPK inhibitor with activity against FLT3-ITD secondary mutations potently inhibits acute myeloid leukemia cell lines. *Future Med Chem*. 2018;10(7):823-835. doi:10.4155/fmc-2017-0298
43. Lebedev TD, Vagapova ER, Popenko VI, Leonova OG, Spirin P V., Prassolov VS. Two receptors, two isoforms, two cancers: Comprehensive analysis of kit and trka expression in neuroblastoma and acute myeloid leukemia. *Front Oncol*. 2019;9(OCT):1046. doi:10.3389/fonc.2019.01046
44. Joshi SK, Qian K, Bisson WH, et al. Discovery and characterization of targetable NTRK point mutations in hematologic neoplasms. *Blood*. 2020;135(24):2159-2170. doi:10.1182/blood.2019003691
45. Herbrich SM, Kannan S, Nolo RM, Hornbaker M, Chandra J, Zweidler-McKay PA. Characterization of TRKA signaling in acute myeloid leukemia. *Oncotarget*. 2018;9(53):30092-30105. doi:10.18632/oncotarget.25723
46. Taylor J, Pavlick D, Yoshimi A, et al. Oncogenic TRK fusions are amenable to inhibition in hematologic malignancies. *J Clin Invest*. 2018;128(9):3819-3825. doi:10.1172/JCI120787
47. Lindsay RM. Role of neurotrophins and trk receptors in the development and maintenance of sensory neurons: An overview. *Philos Trans R Soc B Biol Sci*. 1996;351(1338):365-373. doi:10.1098/rstb.1996.0030
48. Herrmann JL, Menter DG, Hamada JI, Marchetti D, Nakajima M, Nicolson GL. Mediation of NGF-stimulated extracellular matrix invasion by the human melanoma low-affinity p75 neurotrophin receptor: Melanoma p75 functions independently of trkA. *Mol Biol Cell*. 1993;4(11):1205-1216. doi:10.1091/mbc.4.11.1205
49. Kizilyer A, Singh M V., Singh VB, Suwunnakorn S, Palis J, Maggirwar SB. Inhibition of Tropomyosin Receptor Kinase A Signaling Negatively Regulates Megakaryopoiesis and induces Thrombopoiesis. *Sci Rep*. 2019;9(1):1-15. doi:10.1038/s41598-019-39385-x

50. Smith KM, Fagan PC, Pomari E, et al. Antitumor activity of entrectinib, a pan-TRK, ROS1, and ALK inhibitor, in ETV6-NTRK3-positive acute myeloid leukemia. *Mol Cancer Ther*. 2018;17(2):455-463. doi:10.1158/1535-7163.MCT-17-0419

51. Jiang T, Wang G, Liu Y, et al. Development of small-molecule tropomyosin receptor kinase (TRK) inhibitors for NTRK fusion cancers. *Acta Pharm Sin B*. 2021;11(2):355-372. doi:10.1016/j.apsb.2020.05.004

52. Rolfo C, Ruiz R, Giovannetti E, et al. Entrectinib: A potent new TRK, ROS1, and ALK inhibitor. *Expert Opin Investig Drugs*. 2015;24(11):1493-1500. doi:10.1517/13543784.2015.1096344

53. Federman N, McDermott R. Larotrectinib, a highly selective tropomyosin receptor kinase (TRK) inhibitor for the treatment of TRK fusion cancer. *Expert Rev Clin Pharmacol*. 2019;12(10):931-939. doi:10.1080/17512433.2019.1661775

54. Manley PW, Caravatti G, Furet P, et al. Comparison of the Kinase Profile of Midostaurin (Rydapt) with That of Its Predominant Metabolites and the Potential Relevance of Some Newly Identified Targets to Leukemia Therapy. *Biochemistry*. 2018;57(38):5576-5590. doi:10.1021/ACS.BIOCHEM.8B00727/SUPPL_FILE/BI8B00727_SI_001.PDF

55. George DJ, Dionne CA, Jani J, et al. Sustained in Vivo Regression of Dunning H Rat Prostate Cancers Treated with Combinations of Androgen Ablation and Trk Tyrosine Kinase Inhibitors, CEP-751 (KT-6587) or CEP-701 (KT-5555). *Cancer Res*. 1999;59(10):2395 LP - 2401. http://cancerres.aacrjournals.org/content/59/10/2395.abstract.

56. Smith CC, Lasater EA, Lin KC, et al. Crenolanib is a selective type I pan-FLT3 inhibitor. *Proc Natl Acad Sci*. 2014;111(14):5319 LP - 5324. doi:10.1073/pnas.1320661111

57. O'Hare T, Shakespeare WC, Zhu X, et al. AP24534, a Pan-BCR-ABL Inhibitor for Chronic Myeloid Leukemia, Potently Inhibits the T315I Mutant and Overcomes Mutation-Based Resistance. *Cancer Cell*. 2009;16(5):401-412. doi:10.1016/J.CCR.2009.09.028/ATTACHMENT/3E40F350-67E2-4719-9F71-74C24F3BCE9A/MMC1.PDF

58. Chan WW, Wise SC, Kaufman MD, et al. Conformational Control Inhibition of the BCR-

ABL1 Tyrosine Kinase, Including the Gatekeeper T315I Mutant, by the Switch-Control Inhibitor DCC-2036. *Cancer Cell*. 2011;19(4):556-568. doi:10.1016/J.CCR.2011.03.003/ATTACHMENT/37A6E583-8A34-48F1-8BB7-A453992742F5/MMC1.PDF

59. Cortes JE, Khaled S, Martinelli G, et al. Quizartinib versus salvage chemotherapy in relapsed or refractory FLT3-ITD acute myeloid leukaemia (QuANTUM-R): a multicentre, randomised, controlled, open-label, phase 3 trial. *Lancet Oncol*. 2019;20(7):984-997. doi:10.1016/S1470-2045(19)30150-0
60. Aikawa T, Togashi N, Iwanaga K, et al. Quizartinib, a selective FLT3 inhibitor, maintains antileukemic activity in preclinical models of RAS-mediated midostaurin-resistant acute myeloid leukemia cells. *Oncotarget*. 2020;11(11):943-955. doi:10.18632/oncotarget.27489
61. Fletcher L, Joshi SK, Traer E. Profile of quizartinib for the treatment of adult patients with relapsed/refractory FLT3-ITD-positive acute myeloid leukemia: Evidence to date. *Cancer Manag Res*. 2020;12:151-163. doi:10.2147/CMAR.S196568
62. Galanis A, Levis M. Inhibition of c-kit by tyrosine kinase inhibitors. *Haematologica*. 2015;100(3):E77-E79. doi:10.3324/haematol.2014.117028
63. Warkentin AA, Lopez MS, Lasater EA, et al. Overcoming myelosuppression due to synthetic lethal toxicity for FLT3-targeted acute myeloid leukemia therapy. *Elife*. 2014;3. doi:10.7554/eLife.03445
64. Xu Y, Wang NY, Song XJ, et al. Discovery of novel N-(5-(tert-butyl)isoxazol-3-yl)-N'-phenylurea analogs as potent FLT3 inhibitors and evaluation of their activity against acute myeloid leukemia in vitro and in vivo. *Bioorg Med Chem*. 2015;23(15):4333-4343. doi:10.1016/J.BMC.2015.06.033
65. Cheng C, Liu B, Zhang Y, Long B, Zhang W. Preparation of substituted urea derivatives for modulating the FLT3 kinase activity and inhibiting FLT3-ITD. *PCT Int Appl*. 2015;(WO2015043492A1):118pp.
66. Si J, Jiang M. Preparation of urea compounds as antitumor agents. *PCT Int Appl*. 2017;(WO2017152874A1):155pp.; Chemical Indexing Equivalent to 167:431507.

67. Zorn JA, Wang Q, Fujimura E, Barros T, Kuriyan J. Crystal structure of the FLT3 kinase domain bound to the inhibitor quizartinib (AC220). *PLoS One*. 2015;10(4). doi:10.1371/journal.pone.0121177

68. Zhou Q, Reekie TA, Abbassi RH, et al. Synthesis and in vitro evaluation of diverse heterocyclic diphenolic compounds as inhibitors of DYRK1A. *Bioorganic Med Chem*. 2018;26(22):5852-5869. doi:10.1016/j.bmc.2018.10.034

69. Dokla EME, Fang CS, Abouzid KAM, Chen CS. 1,2,4-Oxadiazole derivatives targeting EGFR and c-Met degradation in TKI resistant NSCLC. *Eur J Med Chem*. 2019;182:111607. doi:10.1016/j.ejmech.2019.111607

70. Palmer BD. Structure-activity relationships for 1-phenylbenzimidazoles as selective ATP site inhibitors of the platelet-derived growth factor receptor. *J Med Chem*. 1998;41(27):5457-5465. doi:10.1021/jm9804681

71. Bilodeau MT, Cunningham AM, Koester TJ, et al. Design and synthesis of 1,5-diarylbenzimidazoles as inhibitors of the VEGF-receptor KDR. *Bioorganic Med Chem Lett*. 2003;13(15):2485-2488. doi:10.1016/S0960-894X(03)00485-2

72. Smith CC, Lin K, Stecula A, Sali A, Shah NP. FLT3 D835 mutations confer differential resistance to type II FLT3 inhibitors. *Leukemia*. 2015;29(12):2390-2392. doi:10.1038/leu.2015.165

73. Kennedy VE, Smith CC. FLT3 Mutations in Acute Myeloid Leukemia: Key Concepts and Emerging Controversies. *Front Oncol*. 2020;10. doi:10.3389/fonc.2020.612880

74. Daver N, Schlenk RF, Russell NH, Levis MJ. Targeting FLT3 mutations in AML: review of current knowledge and evidence. *Leukemia*. 2019;33(2):299-312. doi:10.1038/s41375-018-0357-9

75. Makishima H, Sugimoto Y, Szpurka H, et al. CBL mutation-related patterns of phosphorylation and sensitivity to tyrosine kinase inhibitors. *Leukemia*. 2012;26(7):1547-1554. doi:10.1038/leu.2012.7

76. Hu S, Niu H, Minkin P, et al. Comparison of antitumor effects of multitargeted tyrosine kinase inhibitors in acute myelogenous leukemia. *Mol Cancer Ther*. 2008;7(5):1110-1120. doi:10.1158/1535-7163.MCT-07-2218

77. Shimada K, Hayano M, Pagano NC, Stockwell BR. Cell-Line Selectivity Improves the Predictive Power of Pharmacogenomic Analyses and Helps Identify NADPH as Biomarker for Ferroptosis Sensitivity. *Cell Chem Biol*. 2016;23(2):225-235. doi:10.1016/j.chembiol.2015.11.016

78. Ion GND, Nitulescu GM. In search of outliers. Mining for protein kinase inhibitors based on their anti-proliferative NCI-60 cell lines profile. *Molecules*. 2020;25(8). doi:10.3390/molecules25081766

79. Ardini E, Bosotti R, Borgia AL, et al. The TPM3-NTRK1 rearrangement is a recurring event in colorectal carcinoma and is associated with tumor sensitivity to TRKA kinase inhibition. *Mol Oncol*. 2014;8(8):1495-1507. doi:10.1016/j.molonc.2014.06.001

80. Nogami A, Watanabe D, Okada K, et al. FLT3-ITD Enhances Proliferation and Survival of AML Cells through Activation of RSK1 to Upregulate the mTORC1/eIF4F Pathway Cooperatively with PIM or PI3K and to Inhibit Bad and Bim. *Blood*. 2019;134(Supplement_1):1425-1425. doi:10.1182/blood-2019-123183

81. Peschel I, Podmirseg SR, Taschler M, et al. FLT3 and FLT3-ITD phosphorylate and inactivate the cyclin-dependent kinase inhibitor p27Kip1 in acute myeloid leukemia. *Haematologica*. 2017;102(8):1378-1389. doi:10.3324/haematol.2016.160101

82. Wang ES, Baron J. Management of toxicities associated with targeted therapies for acute myeloid leukemia: When to push through and when to stop. *Hematol (United States)*. 2020;20(1):57-66. doi:10.1182/HEMATOLOGY.2020000089

83. Abdel-Aziz AK, Abdel-Naim AB, Shouman S, Minucci S, Elgendy M. From resistance to sensitivity: Insights and implications of biphasic modulation of autophagy by sunitinib. *Front Pharmacol*. 2017;8(OCT):718. doi:10.3389/fphar.2017.00718

84. Aqsa A, Droubi S, Amarnath S, Al-Moussawi H, Abergel J. Sunitinib-Induced Acute Liver Failure. *Case Rep Gastroenterol*. 2021;15(1):17-21. doi:10.1159/000511249

85. Gadaleta-Caldarola G, Divella R, Mazzocca A, et al. Sorafenib: The gold standard therapy in advanced hepatocellular carcinoma and beyond. *Futur Oncol*. 2015;11(16):2263-2266. doi:10.2217/fon.15.161

86. Abdel-Aziz AK, Pallavicini I, Ceccacci E, et al. Tuning mTORC1 activity dictates the

response to LSD1 inhibition of acute myeloid leukemia. *Haematologica*. 2020;105(8):2105-2117. doi:10.3324/haematol.2019.224501

87. Abdel-Aziz AK, Minucci S. Comparing apples with oranges: Studying LSD1 inhibitors in cellular assays. *Pharmacol Res*. 2019;146. doi:10.1016/j.phrs.2019.104345

88. Abdel-Aziz AK, Azab SSE, Youssef SS, El-Sayed AM, El-Demerdash E, Shouman S. Modulation of imatinib cytotoxicity by selenite in HCT116 colorectal cancer cells. *Basic Clin Pharmacol Toxicol*. 2015;116(1):37-46. doi:10.1111/bcpt.12281

89. Dokla EME, Abdel-Aziz AK, Milik SN, et al. Indolin-2-one derivatives as selective Aurora B kinase inhibitors targeting breast cancer. *Bioorg Chem*. 2021;117:105451. doi:10.1016/J.BIOORG.2021.105451

90. Abdel-Aziz AK, Shouman S, El-Demerdash E, Elgendy M, Abdel-Naim AB. Chloroquine synergizes sunitinib cytotoxicity via modulating autophagic, apoptotic and angiogenic machineries. *Chem Biol Interact*. 2014;217:28-40. doi:10.1016/j.cbi.2014.04.007